Viscosity of Polyelectrolytes Solutions in Nanofilms

ARTICLE *in* LANGMUIR · MARCH 2010

Impact Factor: 4.46 · DOI: 10.1021/la9046676 · Source: PubMed

6 AUTHORS, INCLUDING:

Emmanuelle Rio
Université Paris-Sud 11
55 PUBLICATIONS **547** CITATIONS
SEE PROFILE

Frédéric Restagno
Université Paris-Sud 11
58 PUBLICATIONS **631** CITATIONS
SEE PROFILE

Cagri Üzüm
Surflay Nanotec GmbH
14 PUBLICATIONS **489** CITATIONS
SEE PROFILE

Regine von Klitzing
Technische Universität Berlin
169 PUBLICATIONS **4,129** CITATIONS
SEE PROFILE

Langmuir
Article
pubs.acs.org/Langmuir

Viscosity of Polyelectrolytes Solutions in Nanofilms

Jérôme Delacotte,[†] Emmanuelle Rio,[†] Frédéric Restagno,*[,†] Cagri Uzüm,[‡] Regine von Klitzing,[‡] and Dominique Langevin[†]

[†]*LPS, Université Paris-Sud 11, CNRS UMR 8502, Bât. 510, F-91405 Orsay, and* [‡]*Technische Universität Berlin Institut für Chemie Stranski-Laboratorium, Strasse des 17. Juni 135, D-10623 Berlin*

Received December 11, 2009. Revised Manuscript Received March 5, 2010

We use a thin film pressure balance to probe the rheological properties of thin liquid films. These films are made from mixed aqueous solutions of surfactants and polyelectrolytes. They drain under applied pressure in a noncontinuous way due to a stratification process of the polyelectrolytes network. The stratification kinetics was studied for films stabilized by different surfactants. Using a theoretical model, it is possible to examine the effect of both the surfactant and the film thickness on the local dissipation. On one hand, it was observed that dissipation depends on the polyelectrolyte concentration only, regardless whether the surfactant is neutral or bears electric charges opposite to those of the polyelectrolyte. On the other hand, it was found that dissipation is stronger in thinner films.

Introduction

During recent years the pursuit of scale reduction inherent to nanotechnologies has been extended to the fluidic domain and liquid flow manipulation, with the important development of micro- and nanofluidics.[1] However, reducing the scale of any system leads invariably to an enhancement of the influence of surface properties with respect to the bulk ones: given the scale reduction, most phenomena take place at the boundaries, and a fundamental understanding of how surface properties might affect the overall flow properties has become crucial to the design and optimization of operational devices. Apart from microfluidics, confined liquid flows are widely present in foams. Controlling foam stability is of major importance in a wide variety of industrial sectors with numerous applications such as in cosmetics, food, and new materials.[2] It has long been realized that polymer additives in surfactant solutions can greatly affect the stability of foam. Indeed, most industrial foaming formulations contain at least one type of polymer combined with surfactants to optimize the desired foam properties. The presence of these polymers in the foaming solution were shown to have consequences for the dynamic properties of the resulting foam films.[3,4] In aqueous solutions the polyelectrolyte chains overlap above a critical concentration c^* and form a network. Values above c^* start the so-called semidilute regime. Jumplike discontinuities of disjoining pressure isotherms $\Pi(h)$ (force between surfaces counted per unit area versus film thickness h), were evidenced in the confined geometry of free-standing thin liquid films leading to a film stratification, with a period equal to the mesh size of the polymer network.[4,5] Moreover, the stratification kinetics does not seem simply related to the bulk viscosity of the foaming solution.[6,7] The purpose of this article is to explore further the nature of the viscous dissipation in thin films. As in former work, we study the kinetics of successive stratifications in polyelectrolyte films stabilized by surfactants due to the jumplike discontinuities of disjoining pressure isotherms. The branches where $\partial\Pi/\partial h$ (where Π is the disjoining pressure and h is the film thickness) is positive are unstable so that not all values of h are reachable. Between two authorized thicknesses, a coexistence of thinner and thicker domains is observed (see Figure 1). The kinetics of these stratifications can then be linked to dissipation inside the films.[6,7] Indeed these stratifications have also been observed with lubricant molecules in the surfaces forces apparatus by Mugele et al.,[8] and the dynamics of domain opening has been shown to follow two-dimensional hydrodynamics.

Experimental Details

Materials. For our experiments we used polyacrylamide sulfonate (PAMPS) as polyelectrolyte. This polymer synthesized by SNF Floerger, is a statistical copolymer composed of neutral monomers of acrylamide (AM) and charged monomers of acrylamidomethyl propane sulfonate (AMPS). The studied molecular weight was $M_w = 9.4 \times 10^5$ g·mol^{-1}. One degree of charge was investigated: $x = 50\%$. To eliminate any traces of surfactant molecules and low molecular weight impurities, the polymer solutions were filtered under a pressure of 1.5 bar with a cutoff of 30 kDa. The polymers were then rinsed and freeze-dried. The polymer concentration was varied from 0.3 wt % to 0.4 wt %. Indeed, the concentration must be high enough to observe at least one stratification event and low enough to obtain low viscosity and allow filling of the porous plate. We used two different surfactants, a cationic and a neutral surfactant, to stabilize the films. The cationic surfactant, dodecyltrimethyl ammonium bromide (DTAB) from Aldrich, was recrystallized three times before use. The nonionic surfactant, $C_{12}G_2$ (*n*-dodecyl-β-maltoside, purity >99.5%) from GLYCON Biomedicals was used as delivered. All solutions were prepared with Milli-Q water.

PAMPS and DTAB have opposite charges and form surface complexes which make the surfaces more rigid. Above a certain surfactant concentration called critical aggregation concentration (CAC), bulk complexes also form. In the case of DTAB and PAMPS, in the investigated range of polymer concentrations c_p between 0.3 and 0.4 wt %, the CAC is 10^{-3} mol·L^{-1}. In this work, the surfactant concentration was fixed at 5×10^{-5} mol·L^{-1} well below the CAC, itself well below the critical micellar concentration

*Corresponding author. E-mail: restagno@lps.u-psud.fr.

(1) Whitesides, G. M.; Stroock, A. *Phys. Today* **2001**, *1*, 42.
(2) Prud'homme, R. K.; Khan, S.A. *Foams;* CRC Press: New-York, 1995.
(3) Bergeron, V.; Langevin, D.; Asnacios, A. *Langmuir* **1996**, *12*, 1550−1556.
(4) Asnacios, A.; Espert, A.; Colin, A.; Langevin, D. *Phys. Rev. Lett.* **1997**, *78*, 4974−4977.
(5) Stubenrauch, C.; von Klitzing, R. *J. Phys.: Condens. Matter* **2003**, *15*, R1197−R1232.
(6) Heinig, P.; Beltrán, C. M., Langevin, D. *Phys. Rev. E* **2006**, *73*, 051607.
(7) Beltrán, C. M. Langevin, D. *Phys. Rev. Lett.* **2005**, *94*, 217803.
(8) Becker, T.; Mugele, F. *Phys. Rev. Lett.* **2003**, *91*, 166104.

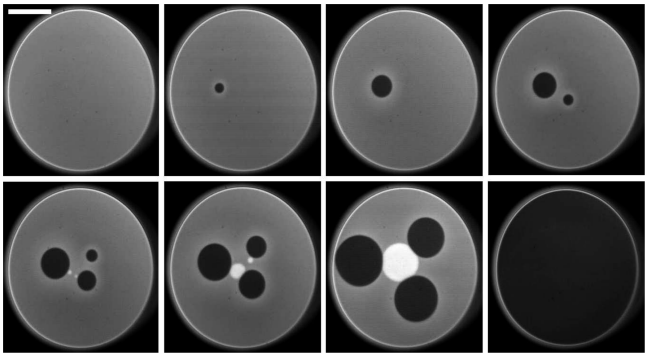

Figure 1. Opening of a thinner domain in a thin film. The black domain is thinner and invades all the thin film. In some cases, when the domain is large enough, the surrounding rim breaks into droplets seen as white circles in the bottom pictures. The scale bar length is 200 μm.

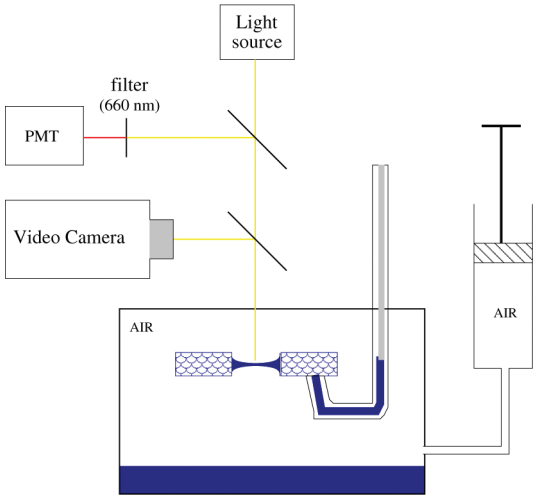

Figure 2. Schematic of the experiment: A thin film is held by a porous plate and observed by video microscopy (videocamera) and by interferometry through a photomultiplier tube (PMT). The pressure is maintained in the sealed cell thanks to a syringe pump.

(CMC, equal to 15×10^{-3} mol·L^{-1}). $C_{12}G_2$ is neutral and adsorbs at the surface without forming surface complexes with the polymer. The surfactant concentration used (5×10^{-5} mol·L^{-1}) was also below the CMC (equal to 0.15×10^{-3} mol·L^{-1}).

The Thin Film Balance Rheometer. The device we used for these experiments is a thin film pressure balance (TFPB) (see Figure 2) which is a modified version of the porous plate technique, first developed by Mysels.[9−11] This device works by maintaining a balance between applied pressure and forces between film surfaces (disjoining pressure). This technique had been used before to study the behavior of other polymers under confinement.[5] The liquid films are formed in a hole drilled through a fritted glass disk which is fused to a 3 mm diameter capillary tube. The film holder is enclosed in a hermetically sealed Plexiglas cell with the capillary tube exposed to a constant reference pressure. Once assembled, the cell is mounted on a vibration-isolation system and the pressure in the cell is regulated with a syringe pump automatically operated through a precise screw driver controlled by a LabVIEW program. The difference between cell pressure and atmospheric pressure is equal to the disjoining pressure at equilibrium. The disjoining pressure in investigated films was around 10 Pa (uncertainty is large at these low pressures, of the order of 10 Pa). The film can be observed using a video-microscope, and film stratification images are recorded. Image analysis allows monitoring the time variation of the radius of thin domains in thicker films. Moreover, the film thickness is measured by the Scheludko's microinterferometric method[12] using a laser light reflected by the film. The experiments have been carried out under ambient light conditions using a chopped laser signal and a lock-in amplifier.

The bulk viscosities of the solutions used have been measured by using a commercial rheometer (Anton Paar Physica MCR 300) equipped with cone/plate geometry. As expected, the polymer solutions exhibit shear-thinning features in the shear rates range from 10 to 500 s^{-1}. Table 1 gives the viscosities at a shear rate $\dot{\gamma}$ = 200 s^{-1} corresponding to the order of magnitude of the shear rate in the thin films during the stratification process.

Table 1. Viscosity of the PAMPS Solutions and AFM Characterization of the Oscillatory Force Inside a Film for Different PAMPS Concentrations[a]

c_p (wt %)	η (mPa·s)	A (nN)	h^* (nm)	$\tilde{h}$ (nm)	$\frac{C}{4D}$
0.20	12.7	0.283	16.6	28.6	0.038
0.30	15.4	0.306	15.4	27.0	0.040
0.35	16.7	0.318	14.0	24.9	0.042
0.40	18.3	0.329	12.2	22.0	0.044

[a] The values of both h^* and $\tilde{h}$ have experimental error of 1 nm; A and $C/(4D)$ are measured with an accuracy of 10%.

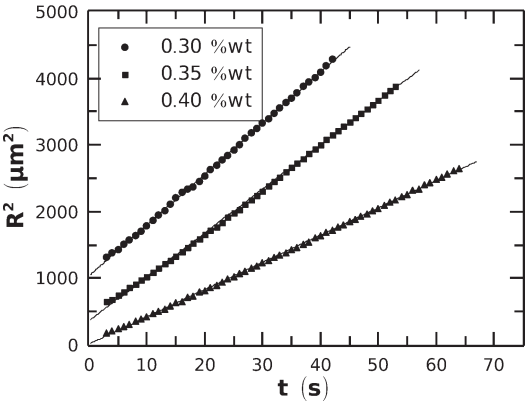

Figure 3. Increase of the domain radius with time. The figure shows the evolution of R for a mixed solution of PAMPS and $C_{12}G_2$ for three different PAMPS concentrations, as given in the insert.

Results

Figure 3 shows the evolution of the square of domain radii with time. It increases linearly with time, as it has already been observed,[6,7] and the slope depends significantly on the polyelectrolyte concentration. Note that we always stop the experiment when droplets appear around the domain due to rim instability (fifth image in Figure 1) after which the opening velocity increases. The opening velocity, related to the change in area with time, is defined as

$$C = \frac{\partial R^2}{\partial t} \tag{1}$$

and has the dimension of a diffusion coefficient.

Most of the time, we observed transitions either from films made of three layers to films made of two layers ($N = 3 \Rightarrow 2$) or

(9) Mysels, K. J.; Jones, M. N. *Discuss. Faraday Soc.* **1966**, *42*, 42−50.
(10) Bergeron, V.; Radke, C. J. *Langmuir* **1992**, *8*, 3020−3026.
(11) Kleinschmidt, F.; Stubenrauch, C.; Delacotte, J.; von Klitzing, R.; Langevin, D. *J. Phys. Chem. B* **2009**, *113*, 3972−3980.
(12) Scheludko, V. A. *Colloid Polym. Sci.* **1957**, *155*, 39−44.

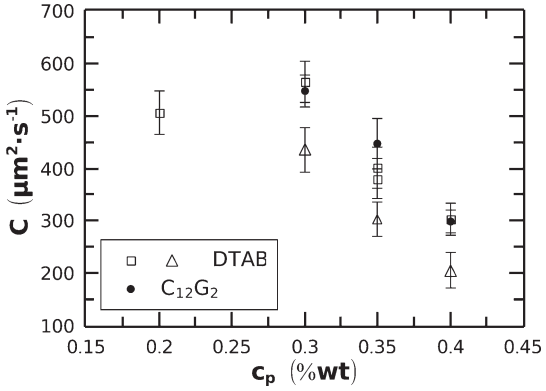

Figure 4. Opening velocity of the domains as a function of polyelectrolyte concentration. Empty triangles and black circles correspond respectively to films stabilized by DTAB and $C_{12}G_2$ (transition $N = 2 \Rightarrow 1$). Empty squares correspond to DTAB and to the transition $N = 3 \Rightarrow 2$. Note that, for a given polyelectrolyte concentration, empty triangles and black circles correspond to films of comparable thickness.

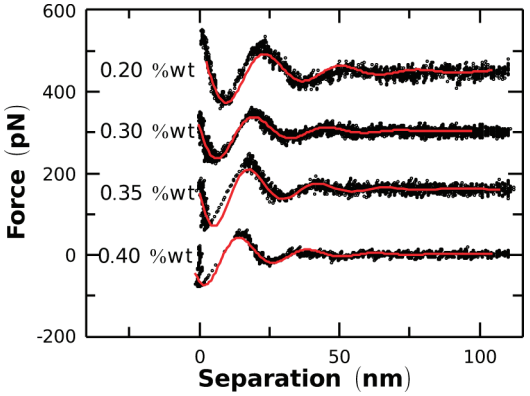

Figure 5. Measurement of the interaction force inside the film as a function of its thickness. The AFM measurement is presented for different PAMPS concentrations. The data have been shifted in the vertical direction for the sake of clarity.

from films made of two layers to films made of 1 layer ($N = 2 \Rightarrow 1$). Both transitions were sometimes consecutively observed in the same film (when rupture has not occurred before the second transition). The main results are presented in Figure 4. The measured opening velocities are plotted for different surfactants and polyelectrolyte concentrations. Note that each point is an average of several experiments (between 2 and 5). This velocity depends on PAMPS concentration, surfactant, and film thickness. At this stage, it is only possible to say that, in films of comparable thickness, the domains seems to open faster when the film is stabilized by $C_{12}G_2$ rather than by DTAB.

In a previous study,[7] it was observed that kinetics of stratification was faster when polyelectrolyte and surfactant carry the same charge. The opening velocity C of the thinner domains was around 3 times higher than for $C_{12}G_2$ and around 6 times higher than for DTAB in the present work. Moreover, C was comparable to the value observed in films made of pure surfactant solution.

In the following we will show that C is also expected to depend on film thickness, disjoining pressure gradient and bulk viscosity η. It is then impossible to interpret the data without a theoretical model. To quantify the dissipation, we will use such a model and rescale the opening velocity taking into account the values of Π, h, and η.

Disjoining Pressure Measurements. Although the TFPB allows the measurement of disjoining pressure, only parts of $\Pi(h)$ are obtained: positive Π, negative $d\Pi/dh$. We therefore used another technique to access the full $\Pi(h)$ curve, necessary for the interpretation of C data.

The colloidal probe technique for disjoining pressure measurements was first developed by Ducker et al.[13] In our experiments, a silica particle is glued with epoxy to a tipless cantilever (Ultrasharp Contact Silicon Cantilevers, CSC12) produced by μMasch. The silica particles are produced by the Bangs Laboratories, Inc., and all have a radius R of about 3.35 μm. The tip is treated by plasma cleaning for 10 min right before each measurement cycle to remove all the organic components on its surface. The substrate used is a silicon wafer with a native SiO_2 top layer, cleaned with the RCA[14] method and stored in Millipore water before use. Just before each experiment, the substrate is taken out of the water and dried in a nitrogen stream. Then a drop of the polymer solution is put onto the substrate, and the probing head is immersed into the solution. In these experiments, no surfactant was used (not needed to stabilize the film). Force versus distance $F(h)$ curves were measured with a commercial atomic force microscope MFP (Molecular Force Probe) produced by Asylum Research, Inc., and distributed by Atomic Force (Mannheim, Germany). Since the distance between the colloidal probe and the substrate is much smaller than the diameter of the probe, the interaction energy per area $E(h)$ can be deduced from the force $F(h)$ using the Derjaguin approximation,[15] $E(h) = F(h)/(2\pi R)$. As both the polymer chains and the SiO_2 surfaces are negatively charged, there is generally no adsorption of polymer onto the surfaces. For each solution, altogether force−distance curves were measured at different lateral positions on the same substrate as well as on different substrates to ensure reproducibility and to get good statistics.

Oscillatory force curves are observed (see Figure 5), and they are fitted by a damped sinusoid:

$$F(h) = A e^{-h/h^*} \sin\left(2\pi \frac{h}{h} + \phi\right) \qquad (2)$$

To measure the disjoining pressure, we differentiate this equation:

$$\Pi(h) = -\frac{\partial E}{\partial h} = -\frac{1}{2\pi R}\frac{\partial F}{\partial h} \qquad (3)$$

where R is the radius of the silica sphere used in the AFM experiment. The parameters A, h, h^*, and ϕ describing the disjoining pressure are summarized in Table 1. In fitting the force−distance data, we have removed points close to hard contact, since additional forces are contributing there. As a consequence, the shift ϕ is not a physically relevant parameter. We checked that the pseudoperiod of the oscillations of the force curves is scaling like $c^{1/2}$ as expected for the network mesh size h^*.[4,16,17] Note that the different parameters are obtained after averaging over more than 30 experiments.

Moreover, it is worth noticing that previous studies[5] showed that the period of oscillatory forces determined using CP-AFM

(13) Ducker, W. A.; Senden, T. J.; Pashley, R. M. *Nature* **1991**, *353*(6341):239−241.
(14) Riegler, H; Engel, M. *Phys. Chem. Chem. Phys.* **1991**, *95*, 1424−1430.
(15) Israelachvili, J. *Intermolecular & Surface Forces,* 2nd ed.; Academic Press: London, 1992.
(16) De Gennes, P.-G.; Pincus, P.; Velasco, R. M.; Brochard, F. *J. Phys. (Paris)* **1976**, *37*, 1461−1473.
(17) Odijk, T. *J. Polym. Sci.* **1977**, *15*, 477−483.

Table 2. Gradient of Disjoining Pressure: For Each Experiment We Report the Polymer Concentration, the Surfactant, the Thickness of the Film before Stratification, the Number N of layers, and the Corresponding $\delta\Pi/\delta h$

c_p (wt %)	surfactant	N	$-\frac{\partial\pi}{\partial h}$ (Pa·nm^{-1})	$h_\infty{}^a$ (nm)	
0.30	DTAB	3 ⟹ 2	13	78	$\tilde{h}$ = 29 nm
0.30	DTAB	2 ⟹ 1	73	49	
0.35	DTAB	3 ⟹ 2	15	86	
0.40	DTAB	3 ⟹ 2	23	77	$\tilde{h}$ = 23 nm
0.40	DTAB	2 ⟹ 1	143	54	
0.30	$C_{12}G_2$	2 ⟹ 1	73	59	
0.35	$C_{12}G_2$	2 ⟹ 1	89	62	
0.40	$C_{12}G_2$	2 ⟹ 1	143	58	

[a] Thicknesses h_∞ are measured with an error of 5%.

agrees very well with the one measured using TFPB, even if boundary conditions are different in both experiments. When we compare $\tilde{h}$ values from Table 1 and Table 2 for polymer concentrations c_p of 0.3 and 0.4 wt %, we see that in both cases, the same values of $\tilde{h}$ (within the experimental error) were obtained with CP-AFM and TFPB, that is 29 and 23 nm for the concentration 0.3 and 0.4 wt %, respectively.

Interpretation

Theoretical Model. The process studied here bears resemblances with dewetting experiments. In a typical dewetting experiment, the driving capillary forces F_d (uncompensated Young force) are balanced by viscous forces F_v (mainly dissipation in the rim surrounding the domain). For nonslipping films, F_v is simply proportional to the viscosity (η) and the velocity (V). In such a case, V is constant in time. Recent experiments on freestanding smectic films by Oswald et al. have shown that when a dislocation loop nucleates, it collapses or grows depending on whether its radius is smaller or larger than a critical value r_c. They measured a constant velocity in thick films and a decrease for thinner films. This dynamics can be explained by the permeation both around the core of the looped dislocation and in the bulk of the meniscus.[18] Studies of thin polymer films on substrates have shown that this is the case when there is no slip at the substrate surface, but that in the presence of slip, the radius of dewetted domains grows as $t^{2/3}$.[19,20] In our experiments, the radius of the domains is neither linear in t, nor proportional to $t^{2/3}$, it is rather proportional to $t^{1/2}$. Similar observations were made by Kralchevski et al.[21] on the kinetics of stratification of foam films containing micelles. They proposed a theory of motion of vacancies which predicts that the velocity depends on the number of domains present at the film surface. This has not been observed in experiments with films containing polyelectrolytes.[6] Other similar observations were made on the wetting behavior of ultrathin stratified polymer films: $R \propto t^{1/2}$.[22] A theory involving molecular forces and molecular friction between the different polymer layers could account for this result. Predictions for the spreading behavior of microscopic droplets were made by de Gennes leading to $R \propto t^{1/2}$,[23] and were confirmed by Heinig et al. on films containing polyelectrolytes, similar to those studied here.[6] Heinig et al. generalized the model of de Gennes to the calculation of the dewetting velocity. This model will be briefly recalled afterward. In the model, the domain expansion is driven by capillary forces as in the more classical dewetting experiments: the film surface tension contains contributions by the disjoining pressure and is lower for thinner films. Dissipation is related to the film viscosity η_{eff}, which can differ from the bulk value in view of confinement effects. The model uses lubrication approximation with no-slip boundary conditions at the surface of the film and leads to

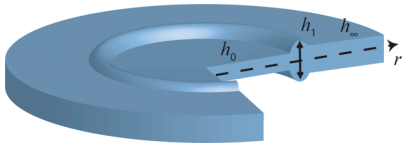

Figure 6. Cross section of an expanding thinner domain of thickness h_0, surrounded by a rim of thickness h_1, in a film of initial thickness h_∞.

$$\frac{\partial h}{\partial t} = \frac{h^3}{12\eta_{eff} r}\frac{\partial}{\partial r}\left(r\frac{\partial P}{\partial r}\right) \tag{4}$$

where the pressure P in the film is obtained with a linear approximation for the disjoining pressure, for $h \simeq h_\infty$

$$P = P_{air} - \frac{\partial\pi}{\partial h}(h - h_\infty) \tag{5}$$

Equation 4 then become a diffusion equation:

$$\frac{\partial h}{\partial t} = D\frac{1}{r}\frac{\partial}{\partial r}\left(r\frac{\partial h}{\partial r}\right) \tag{6}$$

where D is a diffusive coefficient defined by[23]

$$D = -\frac{h_\infty^3}{12\eta_{eff}}\frac{\partial\pi}{\partial h} \tag{7}$$

The integration of eq 6 allows the relation of the diffusive coefficient D to the opening velocity $C = \partial R^2/\partial t$, which is the measured parameter. One obtains[6]

$$\frac{C}{4D} \simeq \frac{h_1 - h_\infty}{h_\infty - h_0}\frac{0.785}{\ln\dfrac{h_\infty - h_0}{h_1 - h_\infty}} \tag{8}$$

where h_∞ is the film thickness far from the opening domain, h_0 the thickness inside, and h_1 the thickness at the boundary of thin and thick films (see Figure 6). Heinig et al. illustrated the difference between C and D by measuring relaxations of small droplets at the surface of the film.[6]

Effective Viscosity Determination. After measuring C, we obtain D from eq 8 and, then, the effective viscosity η_{eff}. $\partial\Pi/\partial h$ can be calculated from the double derivative of the force F, using the parameters of Table 1. During stratification we measured the thickness h of the film. We can then deduce on which stable branch of the disjoining pressure we are. The disjoining pressure gradient is calculated in the region of steepest slope. The AFM and TFPB curves are shifted along the horizontal axis, but we know on which branch we are. The disjoining pressure at which the transition occurs is not zero. We then did the approximation that the slope $\partial\Pi/\partial h$ is the same all along the branch (this is reasonably accurate provided the applied pressure is not too close

(18) Oswald, P.; Picano, F.; Caillier, F. *Phys. Rev. E* **2003**, *68*, 061701.
(19) Redon, C.; , Brzoska, J. B.; , F. Brochard-Wyart. Dewetting and slippage of microscopic polymer-films. *Macromolecules* **1994**, *27*, 468−471.
(20) Reiter, G.; Khanna, R. *Langmuir* **2000**, *16*, 6351−6357.
(21) Kralchevsky, P. A.; Nikolov, A. D.; Wasan, D. T.; , Ivanov, I. B. *Langmuir* **1990**, *6*, 1180−1189.
(22) Valignat, M. P.; Oshanin, G.; Villette, S.; Cazabat, A. M.; Moreau, M. *Phys. Rev. Lett.* **1998**, *80*, 5377−5380.
(23) Joanny, J. F.; de Gennes, P.-G. *C. R. Acad. Sci.* **1984**, *299*, 279−283.

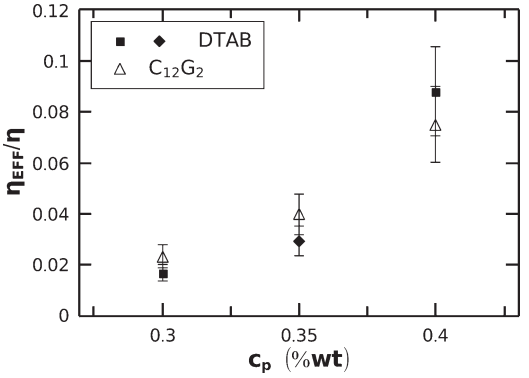

Figure 7. Ratio of the viscosity measured by the TFPB rheometer and the bulk viscosity for the two surfactants.

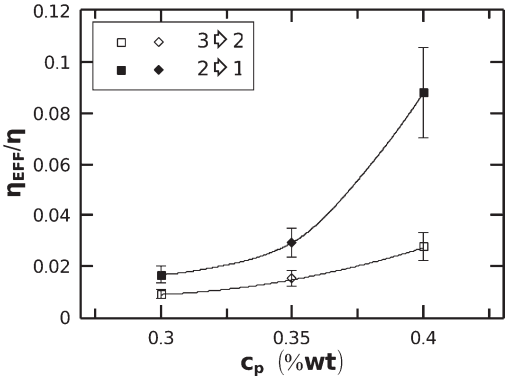

Figure 8. Ratio of the viscosity measured by the TFPB rheometer and the bulk viscosity for two different stratifications. The used surfactant is DTAB. Diamonds correspond to concentration in DTAB of 5×10^{-4} mol·L^{-1} instead of 5×10^{-5} mol·L^{-1} for the square. Black lines are eye-guides.

to the disjoining pressure maxima) and took the maximum value as the linear approximation. Note that $\partial\Pi/\partial h$ depends on the number of film layers. Results are summarized in Table 2.

The calculation of D from the experimental parameter C requires knowledge of the value of $h_1 - h_\infty$ (see eq 8). For this purpose, we use the disjoining pressure variation through the following equation:[6]

$$h_1 - h_\infty = \frac{\tilde{h}}{(\tilde{h}/h^*)^2 + 4\pi^2}(e^{\tilde{h}/h^*} - 1) \qquad (9)$$

According to eq 9, expected values of $h_1 - h_\infty$ are around 3 nm. We checked experimentally that it was consistent with the rim height: the interferometric measurement of the thickness across the rim did not show a meaningful increase compared to the surrounding film, the accuracy of these measurements being of the order of a few nm. D can then be calculated from eq 8 and rescaled by $(h_\infty^3/\eta)(\partial\Pi/\partial h)$ (where η is the bulk viscosity). The values of $C/(4D)$ ratios are reported in Table 1, and effective viscosities are plotted in Figure 7. Note that in this graphic, we plotted only the results of the stratification $2 \Rightarrow 1$. If there were no other dissipation mechanism than the bulk viscosity, η_{eff} should be constant. Effective viscosities measured in thin films stabilized with DTAB and $C_{12}G_2$ are similar. This reveals a noticeable feature: the boundary conditions are not modified by using either a neutral surfactant or a surfactant bearing a charge opposite to that of polyelectrolyte. Indeed, we could have expected a different behavior, since films made with DTAB are stabilized by a mixed monolayer of DTAB/PAMPS at the film surface. Note that, such a low concentration of DTAB (5×10^{-5} mol·L^{-1}) would not allow the stabilization of the film without the polymer. Moreover, we can notice that effective viscosities in thin films are lower (more than 1 order of magnitude) than bulk ones. This suggests that the chain mobility is enhanced in a confined geometry with respect to to the bulk case, as already reported by Beltrán et al. in ref 7. Finally, if we now compare the effective viscosities with the viscosity of water, we observe that the viscosities are lower. This suggests that a more complicated model using either a slip at the liquid−gas interface or an interfacial layer with a lower viscosity should be necessary to get access to the real viscosity of the confined fluid. Furthermore, an underestimation of the disjoining pressure could contribute to decrease the values of effective viscosities. Nevertheless our measurement give us access to a global and averaged viscosity. As a consequence the effect of both the surfactant and the confinement are clear even if the absolute values of the viscosities should be discussed.

In Figure 8, the comparison between the kinetics of $3 \Rightarrow 2$ and $2 \Rightarrow 1$ stratifications observed on films stabilized by DTAB can be observed. The effective viscosity is higher for the second stratification which shows that the dissipation increases upon confinement. It appears that the thinner the film, the higher the dissipation.

As a concluding remark, we note that the effective viscosity increases with polyelectrolyte concentration, as could be expected. Nevertheless, as can be seen in Figure 8, when the film is thick enough, the effective viscosity is less sensitive to concentration variations.

Conclusion

We used an indirect technique to measure the dissipation in thin films of mixed surfactants and polyelectrolytes. The chosen hydrodynamic model allowed us to extract an effective viscosity from stratification kinetics. Our experiments show that without a careful data treatment, the conclusions can be biased. In Figure 4, the opening velocity is different for both surfactants, but Figure 7 shows that the difference is fully accounted for by the difference in disjoining pressure gradient. The data analysis reveals the importance of the confinement which cannot be inferred from the parameter C alone. We show here that the effective viscosity does not depend on the stabilizing surfactant, confirming that the boundary condition is the same. We were able to show that the confinement has a strong effect on dissipation, when polyelectrolyte concentration is high enough: the dissipation is higher in thinner films. It is important to keep in mind that our analysis makes some strong assumptions about the role of the interfaces in hydrodynamic boundary conditions. We plan to investigate further the polyelectrolyte mobility in thin films by using the fluorescence correlation spectroscopy technique[24] and the dynamic surface force apparatus [25] which both allows a direct access to the slippage length and the local viscosity. In parallel, this work will be extended to other polymers−surfactant mixtures and related to film drainage and rupture.

Acknowledgment. We want to thank Yan Zeng for her help on AFM measurements, and one referee whose relevant comments allowed improvement of this article.

(24) Joly, L.; Ybert, C.; Bocquet, L. *Phys. Rev. Lett.* **2006**, *96*, 046101.
(25) Restagno, F.; Crassous, J.; Charlaix, E.; Cottin-Bizonne, C.; Monchanin, M. *Rev. Sci. Instrum.* **2002**, *73*, 2292−2297.